PHYSICAL REVIEW D **74,** 114006 (2006)

Thermal dilepton production from dropping ρ based on the vector manifestation

Masayasu Harada[1] and Chihiro Sasaki[2]
[1]*Department of Physics, Nagoya University, Nagoya, 464-8602, Japan*
[2]*Gesellschaft für Schwerionenforschung (GSI), 64291 Darmstadt, Germany*
(Received 21 August 2006; published 12 December 2006)

We study the pion electromagnetic form factor and the dilepton production rate in hot matter using the hidden local symmetry theory as an effective field theory for pions and ρ mesons. In this framework, the chiral symmetry restoration is realized as the vector manifestation (VM) in which the massless vector meson becomes the chiral partner of the pion, giving a theoretical support to the dropping ρ à la Brown-Rho scaling. In the VM, the vector dominance (VD) is strongly violated near the phase transition point associated with the dropping ρ. We show that the effect of the violation of the VD substantially suppresses the dilepton production rate compared with the one predicted by assuming the VD together with the dropping ρ.

DOI: 10.1103/PhysRevD.74.114006 PACS numbers: 12.39.Fe, 12.40.Vv

I. INTRODUCTION

Changes of hadron properties are indications of chiral symmetry restoration occurring in hot and/or dense QCD and have been explored using various effective chiral approaches [1,2]. Dileptons are considered to be promising probes since they pass through the fireball created in heavy-ion collisions without further interactions and must carry information on the modifications of hadrons in matter. The short-lived vector mesons like the ρ mesons are expected to decay into dileptons inside the hot/dense matter. The dilepton production around the vector meson resonances mainly come from two-pion processes. An enhancement of dielectron mass spectra below the ρ/ω resonance was first observed at CERN SPS [3] and it is an indication of the medium modification of the vector mesons.

The vector meson mass in matter still remains an open issue. Although there are several scenarios like collisional broadening due to interactions with the surrounding hot/dense medium [2], and dropping ρ meson mass associated with chiral symmetry restoration [4,5], no conclusive distinction between them has been done. Dropping masses of hadrons following the Brown-Rho (BR) scaling [4] can be one of the most prominent candidates of the strong signal of melting quark condensate $\langle\bar{q}q\rangle$ which is an order parameter of spontaneous chiral symmetry breaking.

The vector manifestation (VM) [5] is a novel pattern of the Wigner realization of chiral symmetry in which the ρ meson becomes massless degenerate with the pion at the chiral phase transition point. The VM is formulated [6–8] in the effective field theory (EFT) based on the hidden local symmetry (HLS) [9,10]. The VM gives a theoretical description of the dropping ρ mass, which is protected by the existence of the fixed point (VM fixed point).

The dropping mass is supported by the mass shift of the ω meson in nuclei measured by the KEK-PS E325 experiment [11] and the CBELSA/TAPS Collaboration [12] and also that of the ρ meson observed in the STAR experiment [13]. Recently, the NA60 Collaboration has provided data for the dimuon spectrum [14] and it seems difficult to explain the data by a naive dropping ρ [15]. However, there are still several ambiguities which are not considered [16–18]. In particular, the strong violation of the vector dominance (VD), which is one of the significant predictions of the VM [19], plays an important role [16] in explaining the data.

In this paper, we shall focus on the dilepton production from the dropping ρ based on the VM using the HLS theory at finite temperature. In the formulation of the VM, an essential role is played by the *intrinsic temperature/density effects* of the parameters which are introduced through the matching to QCD in the Wilsonian sense combined with the renormalization group equations (RGEs). We first study how the *intrinsic temperature/density effects* affect to the dilepton spectra by comparing the predictions of the VM with the ones obtained without intrinsic effects. We next pay special attention to the effect of the violation of the vector dominance (indicated by "$\not{\text{VD}}$") which is also due to the intrinsic effects. We make a comparison between the dilepton production rates predicted by the VM and the ones by the dropping ρ with the assumption of the vector dominance. Our result shows that the effect of the $\not{\text{VD}}$ substantially suppresses the dilepton production rate compared with the one predicted by assuming the VD together with the dropping ρ.

This paper is organized as follows. In Sec. II we give a brief review of the HLS theory and basics of the VM in matter. In Sec. III we determine the temperature dependences of the parameters through the matching and RGEs. Using those in-medium parameters, the form factor and dilepton production rate are studied in Sec. IV. There, a comparison of the predictions of the VM with those assuming the VD together with the dropping ρ is also made. A brief summary and discussions are given in Sec. V.

II. HLS THEORY AND VECTOR MANIFESTATION

In this section, we briefly review the HLS [9,10] and the notion of the VM of chiral symmetry following Refs. [6,20].

A. Hidden local symmetry

The HLS Lagrangian is based on the $G_{\rm global} \times H_{\rm local}$ symmetry, where $G = SU(N_f)_L \times SU(N_f)_R$ is the chiral symmetry and $H = SU(N_f)_V$ is the HLS. The basic quantities are the HLS gauge boson and two matrix valued variables $\xi_L(x)$ and $\xi_R(x)$ which transform as

$$\xi_{L,R}(x) \to \xi'_{L,R}(x) = h(x)\xi_{L,R}(x)g^\dagger_{L,R}, \tag{2.1}$$

where $h(x) \in H_{\rm local}$ and $g_{L,R} \in [SU(N_f)_{L,R}]_{\rm global}$. These variables are parametrized as

$$\xi_{L,R}(x) = e^{i\sigma(x)/F_\sigma} e^{\mp i\pi(x)/F_\pi}, \tag{2.2}$$

where $\pi = \pi^a T_a$ denotes the pseudoscalar Nambu-Goldstone (NG) bosons associated with the spontaneous symmetry breaking of $G_{\rm global}$ chiral symmetry, and $\sigma = \sigma^a T_a$ denotes the NG bosons associated with the spontaneous breaking of $H_{\rm local}$. This σ is absorbed into the HLS gauge boson through the Higgs mechanism, and the gauge boson acquires its mass. F_π and F_σ are the decay constants of the associated particles. The phenomenologically important parameter a is defined as

$$a = \frac{{F_\sigma}^2}{{F_\pi}^2}. \tag{2.3}$$

The covariant derivatives of $\xi_{L,R}$ are given by

$$\begin{aligned} D_\mu \xi_L &= \partial_\mu \xi_L - iV_\mu \xi_L + i\xi_L \mathcal{L}_\mu, \\ D_\mu \xi_R &= \partial_\mu \xi_R - iV_\mu \xi_R + i\xi_R \mathcal{R}_\mu, \end{aligned} \tag{2.4}$$

where V_μ is the gauge field of $H_{\rm local}$, and $\mathcal{L}_\mu$ and $\mathcal{R}_\mu$ are the external gauge fields introduced by gauging $G_{\rm global}$ symmetry.

In the framework of the HLS, it is possible to perform the systematic derivative expansion including the vector mesons as the HLS gauge bosons in addition to the pseudoscalar mesons as the NG bosons [6,21–23]. In this chiral perturbation theory (ChPT) with the HLS, the Lagrangian with lowest derivative terms is counted as $\mathcal{O}(p^2)$, which, in the chiral limit, is given by [9,10]

$$\begin{aligned} \mathcal{L}_{(2)} &= {F_\pi}^2 \,\mathrm{tr}[\hat{\alpha}_{\perp\mu}\hat{\alpha}^\mu_\perp] + {F_\sigma}^2 \,\mathrm{tr}[\hat{\alpha}_{\parallel\mu}\hat{\alpha}^\mu_\parallel] \\ &\quad - \frac{1}{2g^2}\,\mathrm{tr}[V_{\mu\nu}V^{\mu\nu}], \end{aligned} \tag{2.5}$$

where g is the HLS gauge coupling, $V_{\mu\nu}$ is the field strength of V_μ, and

$$\begin{aligned} \hat{\alpha}^{\ \mu}_\perp &= \frac{1}{2i}[D^\mu \xi_R \cdot \xi_R^\dagger - D^\mu \xi_L \cdot \xi_L^\dagger], \\ \hat{\alpha}^\mu_\parallel &= \frac{1}{2i}[D^\mu \xi_R \cdot \xi_R^\dagger + D^\mu \xi_L \cdot \xi_L^\dagger]. \end{aligned} \tag{2.6}$$

There are 35 terms of $\mathcal{O}(p^4)$ [6,23] for general number of flavors N_f (32 terms for $N_f = 3$ and 24 for $N_f = 2$). Among them, the following $\mathcal{O}(p^4)$ terms are relevant to the present analysis:

$$\begin{aligned} \mathcal{L}_{(4)} &= z_1 \,\mathrm{tr}[\hat{\mathcal{V}}_{\mu\nu}\hat{\mathcal{V}}^{\mu\nu}] + z_2 \,\mathrm{tr}[\hat{\mathcal{A}}_{\mu\nu}\hat{\mathcal{A}}^{\mu\nu}] \\ &\quad + z_3 \,\mathrm{tr}[\hat{\mathcal{V}}_{\mu\nu}V^{\mu\nu}], \end{aligned} \tag{2.7}$$

where

$$\begin{aligned} \hat{\mathcal{A}}_{\mu\nu} &= \tfrac{1}{2}[\xi_R \mathcal{R}_{\mu\nu}\xi_R^\dagger - \xi_L \mathcal{L}_{\mu\nu}\xi_L^\dagger], \\ \hat{\mathcal{V}}_{\mu\nu} &= \tfrac{1}{2}[\xi_R \mathcal{R}_{\mu\nu}\xi_R^\dagger + \xi_L \mathcal{L}_{\mu\nu}\xi_L^\dagger], \end{aligned} \tag{2.8}$$

with $\mathcal{R}_{\mu\nu}$ and $\mathcal{L}_{\mu\nu}$ being the field strengths of external gauge fields $\mathcal{R}_\mu$ and $\mathcal{L}_\mu$.

B. Wilsonian matching

The Wilsonian matching was proposed as a novel manner to determine the parameters of EFTs from the underlying QCD [24]. It was applied to the HLS theory in a vacuum, which gives several predictions in good agreement with experiments [6,24]. The Wilsonian matching has been applied to study chiral phase transitions at a large number of flavors [5,6] and at finite temperature/density [7,8]. The matching in the Wilsonian sense is performed based on the following general idea: The bare Lagrangian of an EFT is defined at a suitable high energy scale Λ, and the generating functional derived from the bare Lagrangian leads to the same Green's function as that derived from original QCD Lagrangian at Λ. Then the *bare* parameters of the EFT are determined through the Wilsonian matching. In other words, one obtains the bare Lagrangian of the EFT after integrating out the high energy modes, i.e., the quarks and gluons above Λ. The information for the high energy modes is included in the parameters of the EFT.

We first show the basics of the Wilsonian matching in the vacuum. The Wilsonian matching is done by equating the axial-vector and vector current correlators derived from the HLS to those by the operator product expansion (OPE) in QCD at the matching scale Λ. For the validity of the expansion in the HLS, the matching scale Λ must be smaller than the chiral symmetry breaking scale Λ_χ, above which the ChPT with HLS breaks down. On the other hand, the matching scale Λ should be large enough for the validity of the OPE. In Refs. [6,24,25], several choices of Λ around 1.1 GeV were shown to provide good predictions on the low-energy phenomenology related to the ρ meson in real-life QCD.

In the OPE, the axial-vector and vector correlators are expressed as [26]

$$G_A^{(\mathrm{QCD})}(Q^2) = \frac{1}{8\pi^2}\Bigg[-\left(1+\frac{\alpha_s}{\pi}\right)\ln\frac{Q^2}{\mu^2} + \frac{\pi^2}{3}\frac{\langle\frac{\alpha_s}{\pi}G_{\mu\nu}G^{\mu\nu}\rangle}{Q^4} + \frac{\pi^3}{3}\frac{1408}{27}\frac{\alpha_s\langle\bar{q}q\rangle^2}{Q^6}\Bigg],$$
$$G_V^{(\mathrm{QCD})}(Q^2) = \frac{1}{8\pi^2}\Bigg[-\left(1+\frac{\alpha_s}{\pi}\right)\ln\frac{Q^2}{\mu^2} + \frac{\pi^2}{3}\frac{\langle\frac{\alpha_s}{\pi}G_{\mu\nu}G^{\mu\nu}\rangle}{Q^4} - \frac{\pi^3}{3}\frac{896}{27}\frac{\alpha_s\langle\bar{q}q\rangle^2}{Q^6}\Bigg], \tag{2.9}$$

where μ is the renormalization scale. These current correlators in the HLS around the matching scale Λ are well described by the following forms with the bare parameters:

$$G_A^{(\mathrm{HLS})}(Q^2) = \frac{F_\pi^2(\Lambda)}{Q^2} - 2z_2(\Lambda),$$
$$G_V^{(\mathrm{HLS})}(Q^2) = \frac{F_\sigma^2(\Lambda)[1-2g^2(\Lambda)z_3(\Lambda)]}{M_\rho^2(\Lambda)+Q^2} - 2z_1(\Lambda). \tag{2.10}$$

We set the above correlators to be equal to those in Eq. (2.9) at Λ, up until the first derivative, to obtain the Wilsonian matching conditions at zero temperature [24]. Quantum corrections are incorporated into the parameters through the RGEs. Within this framework, several physical quantities in the low-energy region have been studied and the predictions of the Wilsonian matching are in good agreement with experiments. For details, see Refs. [6,24].

For showing a typical prediction of the Wilsonian matching in the vacuum, let us consider the pion electromagnetic form factor. The leading contributions to the pion form factor are shown in Fig. 1. The form factor is expressed as

$$\mathcal{F}(s) = g_{\gamma\pi\pi} + \frac{g_\rho(s)\cdot g_{\rho\pi\pi}}{m_\rho^2 - s - \theta(s-4m_\pi^2)im_\rho\Gamma_\rho(s)}, \tag{2.11}$$

where θ denotes the step function. In the above, $g_{\gamma\pi\pi}$ is the contribution from the direct photon-π-π interaction, and the one remaining is mediated by the ρ meson exchange. The direct photon-π-π coupling constant $g_{\gamma\pi\pi}$ in the HLS is given as

$$g_{\gamma\pi\pi} = 1 - \frac{a(0)}{2}, \tag{2.12}$$

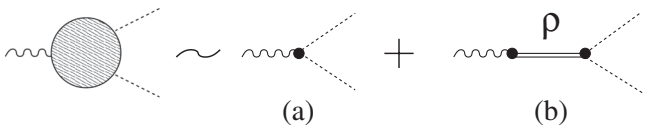

FIG. 1. Leading contributions to the electromagnetic form factor of the pion: (a) the direct $\gamma\pi\pi$ interaction and (b) the $\gamma\pi\pi$ interaction mediated by the ρ meson exchange.

with $a(0)$ being the parameter evaluated at $\mu = 0$. $g_{\rho\pi\pi}$ is the $\rho\pi\pi$ coupling given by

$$g_{\rho\pi\pi} = g(m_\rho)\frac{a(0)}{2}, \tag{2.13}$$

where $g(m_\rho)$ is the HLS gauge coupling at the ρ on shell, $\mu = m_\rho$. $g_\rho(s)$ is the momentum-dependent ρ-γ mixing strength given by

$$g_\rho(s) = \frac{m_\rho^2}{g(m_\rho)} - sg(m_\rho)z_3(m_\rho), \tag{2.14}$$

where $z_3(m_\rho)$ is one of the $\mathcal{O}(p^4)$ parameters given in Eq. (2.7). $\Gamma_\rho(s)$ is the momentum-dependent ρ width given by

$$\Gamma_\rho(s) = \frac{m_\rho}{\sqrt{s}}\left(\frac{s-4m_\pi^2}{m_\rho^2-4m_\pi^2}\right)^{3/2}\Gamma_\rho,$$
$$\Gamma_\rho = \frac{1}{6\pi m_\rho^2}\left(\frac{m_\rho^2-4m_\pi^2}{4}\right)^{3/2}|g_{\rho\pi\pi}|^2. \tag{2.15}$$

We perform the Wilsonian matching as shown in Ref. [6] using the ρ mass, $m_\rho = 775.8$ MeV, and the pion decay constant, $f_\pi = 92.46$ MeV, as inputs and determine the parameters of the HLS as[1]

$$a(0) = 1.94, \qquad g(m_\rho) = 6.02,$$
$$z_3(m_\rho) = -3.87\times10^{-3}, \tag{2.16}$$

for $\Lambda_{\mathrm{QCD}} = 0.4$ GeV and $\Lambda = 1.1$ GeV. In Fig. 2 we show the pion form factor in the timelike region predicted from the Wilsonian matching together with the experimental data obtained from the $e^+e^- \to \pi\pi$ process. We note that an extra peak of the data at $\sqrt{s} \sim 0.78$ GeV is caused by the mixing of the ρ meson with the ω meson due to the small isospin symmetry breaking, which is neglected in the present analysis. It can be seen that the Wilsonian matching well describes the experiment except for the ω region.

Next we apply this procedure to the study of hot/dense matter. As we noted in the beginning of this subsection, the bare parameters are determined by integrating out high frequency modes above the matching scale. Thus, when we integrate out those degrees of freedom in hot/dense matter, the bare parameters are dependent on temperature/density. We shall refer to them as the *intrinsic temperature/density effects* [7,8]. The intrinsic temperature and/or density dependences are nothing but the indication that the hadron has an internal structure constructed from the quarks and gluons. This is similar to the situation where the coupling constants among hadrons are replaced with the momentum-dependent form factor in the high energy region. Thus the intrinsic temperature/density effects play

[1]In Ref. [6], $m_\rho = 771.1$ MeV and the pion decay constant at the chiral limit, $F_\pi(0) = 86.4 \pm 9.7$ MeV, were used as inputs.

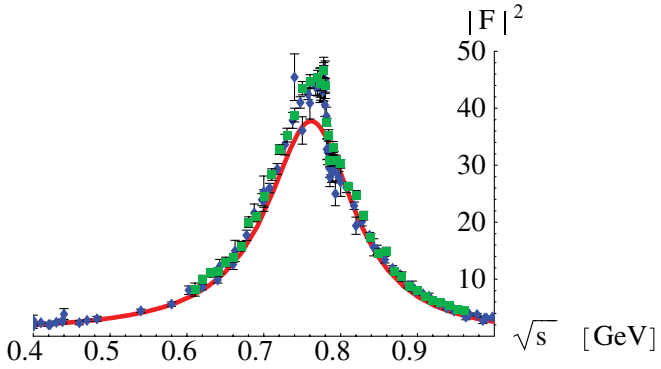

FIG. 2 (color online). Electromagnetic form factor of the pion as a function of the invariant mass $\sqrt{s}$ at zero temperature. The experimental data were taken from Ref. [44] (indicated by $\diamond$) and Ref. [45] (indicated by $\square$).

more important roles in higher temperature/density regions, especially near the phase transition point.

It should be noticed that there is no longer Lorentz symmetry in matter, and the Lorentz nonscalar operators such as $\bar{q}\gamma_\mu D_\nu q$ may exist in the expressions of the OPE current correlators. However, we neglect the contributions from these operators since such effects are suppressed by powers of the matching scale [27,28]. Thus it is a good approximation that we determine the bare parameters at nonzero temperature/density through the matching conditions with putting possible temperature/density dependences on the quark and gluon condensates:

$$\langle\bar{q}q\rangle \to \langle\bar{q}q\rangle_{T,\mu_q}, \qquad \langle G_{\mu\nu}G^{\mu\nu}\rangle \to \langle G_{\mu\nu}G^{\mu\nu}\rangle_{T,\mu_q}. \tag{2.17}$$

Through the matching conditions, the temperature/density dependences of those condensates determine the intrinsic effects of the bare parameters, which are then converted into those of the on-shell parameters through the Wilsonian RGEs.

C. VM in hot/dense matter

The VM was proposed in Ref. [5] as a novel pattern of the Wigner realization of chiral symmetry with a large number of massless quark flavors, in which the vector meson becomes massless at the restoration point and belongs to the same chiral multiplet as the pion, i.e., *the massless vector meson is the chiral partner of the pion*. The studies of the VM in hot/dense matter have been carried out in Refs. [7,8,19,27,28] and the VM was applied to construct an effective Lagrangian for the heavy-light mesons which can describe the recent experimental observation on the $D(0^+, 1^+)$ mesons [29]. We would like to stress that the VD of the electromagnetic form factor of the pion is strongly violated near the critical point associated with the dropping ρ in the VM [19,30]. In the following, we briefly review the VM in hot/dense matter.

We consider the quantity $G_A - G_V$ which is a measure of the spontaneous chiral symmetry breaking in QCD. Here we assume that the quark condensate approaches zero when the restoration point is approached from the broken phase: The phase transition is of second order. In such a case, as we can easily see in Eq. (2.9), $G_A - G_V$ in the OPE approaches zero as

$$G_A^{(\mathrm{QCD})}(Q^2) - G_V^{(\mathrm{QCD})}(Q^2) = \frac{32\pi}{9}\frac{\alpha_s\langle\bar{q}q\rangle^2}{\Lambda^6} \to 0. \tag{2.18}$$

This condition $G_A - G_V \to 0$ should also be satisfied in the EFT. We thus impose that these current correlators approach each other at the bare level, which implies

$$G_A^{(\mathrm{HLS})}(\Lambda; T, \mu_q) - G_V^{(\mathrm{HLS})}(\Lambda; T, \mu_q) \to 0, \tag{2.19}$$

for $(T, \mu_q) \to (T_c, \mu_q^c)$. We require that this equality is satisfied at an arbitrary momentum scale Q near the matching scale Λ. This can be satisfied only when the following conditions for the bare parameters are met:

$$\begin{aligned} g(\Lambda; T, \mu_q) \to 0, \qquad a(\Lambda; T, \mu_q) \to 1, \\ z_1(\Lambda; T, \mu_q) - z_2(\Lambda; T, \mu_q) \to 0, \end{aligned} \tag{2.20}$$

for $(T, \mu_q) \to (T_c, \mu_q^c)$. The first condition immediately implies that the bare ρ mass approaches zero: $M_\rho(\Lambda; T, \mu_q) \to 0$. The second one leads to the agreement of two decay constants: $F_\sigma(\Lambda; T, \mu_q) - F_\pi(\Lambda; T, \mu_q) \to 0$.

We should note that Eq. (2.20) is realized due to the intrinsic T/μ_q effects introduced through the Wilsonian matching. It was shown [6–8] that these conditions are protected by the fixed point of the RGEs [see also Eq. (3.7) in the next section] and never receive quantum corrections at the critical point. Thus the parametric vector meson mass determined at the on shell of the vector meson also vanishes since it is proportional to the vanishing gauge coupling constant. The vector meson mass m_ρ defined as a pole position of the full vector meson propagator has the hadronic corrections through thermal/dense loops, which are proportional to the gauge coupling constant [7,8,19]. Consequently, the vector meson pole mass also goes to zero for $(T, \mu_q) \to (T_c, \mu_q^c)$:

$$m_\rho(T, \mu_q) \to 0. \tag{2.21}$$

By performing the matching to $G_A^{(\mathrm{OPE})} - G_V^{(\mathrm{OPE})}$ near the critical point and using the fact that the vanishing gauge coupling constant is the fixed point of the RGE, we find that *the ρ meson mass drops as the chiral condensate*,

$$m_\rho(T, \mu_q) \propto \langle\bar{q}q\rangle_{T,\mu_q}, \tag{2.22}$$

for $(T, \mu_q) \simeq (T_c, \mu_q^c)$. Note that the Wilsonian matching condition at the critical point provides the nonzero *bare* pion decay constant, $F_\pi^2(\Lambda; T_c, \mu_q^c) \neq 0$, even at the critical point where the on-shell pion decay constant vanishes

by adding the quantum corrections through the RGEs including the quadratic divergences [5] and hadronic temperature/density corrections [7,8].

It has been shown that the VD of the electromagnetic form factor of the pion [31] is accidentally satisfied in $N_f = 3$ QCD at zero temperature and zero density, and that it is strongly violated in large N_f QCD when the VM occurs [30]. The VD is characterized by the direct $\gamma\pi\pi$ being zero. As one can easily see from Eq. (2.12), the VD can be well satisfied when the parameter a is close to 2: $a \simeq 2$. This is actually predicted by the Wilsonian matching in the vacuum as presented in Eq. (2.16). In hot/dense matter, the parameter a is modified by medium effects and approaches unity with increasing T/μ_q toward the critical point, which is due to the intrinsic T/μ_q effects associated with the chiral symmetry restoration [8,19]. This implies that *the VD is strongly violated near the critical point, maximally by 50%*, and it strongly affects the understanding of experiments on the dilepton productions based on the dropping ρ as recently pointed out in Ref. [16]. In the following sections, we will carry out an analysis of the spectral function and the dilepton production rate taking into account the strong violation of the VD.

III. TEMPERATURE DEPENDENCE OF PARAMETERS

Generally, the parameters of EFTs in hot/dense matter have dependences on the temperature/density. This is nothing but the indication that the particles expressed by effective fields are composites of the fundamental degrees of freedom. In the HLS, such dependences (intrinsic temperature/density dependences) can be introduced at the bare level through the Wilsonian matching. The physical quantities in the low-energy region then have two kinds of temperature/density dependences, one is the intrinsic effect and another comes from the ordinary hadronic corrections included through the temperature/density loops. In the following analysis, to determine both effects, we consider the system at finite temperature and zero density.

We consider the intrinsic temperature dependence of the bare parameters of the HLS Lagrangian based on the Wilsonian matching. With increasing temperature toward the critical temperature, the difference of two current correlators in the OPE approaches zero as in Eq. (2.18). Noting that the Wilsonian matching condition obtained from the first derivative of the axial-vector current correlator provides

$$\frac{F_\pi^2(\Lambda;T_c)}{\Lambda^2} = \frac{1}{8\pi^2}\left[1 + \frac{\alpha_s}{\pi}\frac{2\pi^2}{3}\frac{\langle\frac{\alpha_s}{\pi}G_{\mu\nu}G^{\mu\nu}\rangle_{T_c}}{\Lambda^4}\right] \neq 0, \tag{3.1}$$

even at the critical point, we can expand the difference of two correlators $G_A - G_V$ as

$$\begin{aligned} G_A^{(\mathrm{HLS})}(Q^2) - G_V^{(\mathrm{HLS})}(Q^2) \simeq\ & g^2(\Lambda;T)\left(\frac{F_\pi^2(\Lambda;T)}{\Lambda^2}\right)^2 \\ & - (a(\Lambda)-1)\frac{F_\pi^2(\Lambda;T)}{\Lambda^2} \\ & + 2g^2(\Lambda;T)z_3(\Lambda;T)\frac{F_\pi^2(\Lambda;T)}{\Lambda^2} \\ & - 2(z_2(\Lambda;T) - z_1(\Lambda;T)), \end{aligned} \tag{3.2}$$

near the critical point based on the VM. Comparing Eq. (3.2) with Eq. (2.18) and requiring no cancellations among the terms in the right-hand side of Eq. (3.2), we see that both bare g and $a-1$ are proportional to the quark condensate provided by the Wilsonian matching near T_c [7]:

$$g^2(\Lambda;T) \propto \langle\bar{q}q\rangle_T^2, \qquad a(\Lambda;T) - 1 \propto \langle\bar{q}q\rangle_T^2 \quad \text{for } T \simeq T_c. \tag{3.3}$$

This implies that the bare parameters are thermally evolved following the temperature dependence of the quark condensate, which is nothing but the intrinsic temperature effect.

We should note that the above matching conditions hold *only in the vicinity of* T_c: Eq. (3.3) is not valid anymore far away from T_c where ordinary hadronic corrections are dominant. For expressing a temperature above which the intrinsic effect becomes important, we introduce a temperature T_f, the so-called flash temperature [32,33]. The VM and therefore the dropping ρ mass become transparent for $T > T_f$. On the other hand, we expect that the intrinsic effects are negligible in the low-temperature region below T_f: Only hadronic thermal corrections are considered for $T < T_f$. Based on the above consideration, we adopt the following ansatz of the temperature dependences of the bare g and a[2]:

$$\begin{aligned} &\text{for } T < T_f \begin{cases} g(\Lambda;T) = (\text{constant}), \\ a(\Lambda;T) - 1 = (\text{constant}), \end{cases} \\ &\text{for } T > T_f \begin{cases} g(\Lambda;T) \propto \langle\bar{q}q\rangle_T, \\ a(\Lambda;T) - 1 \propto \langle\bar{q}q\rangle_T^2. \end{cases} \end{aligned} \tag{3.4}$$

In the following analysis, we assume that the quark condensates scale as $(T_c - T)^{1/2}$, as in the mean field case for example. Then, the above ansatz in Eq. (3.4) gives the following temperature dependences of the bare g and a, which approach the VM fixed point near T_c:

[2]As was stressed in Refs. [6,20], the VM should be considered only as the limit. So we include the temperature dependences of the parameters only for $T_f < T < T_c - \epsilon$.

$$g(\Lambda;T) = \theta(T_f - T)g(\Lambda;T=0) + \theta(T - T_f) \times g(\Lambda;T=0)\left(1 - \frac{T^2 - T_f^2}{T_c^2 - T_f^2}\right)^{1/2},$$

$$a(\Lambda;T) = \theta(T_f - T)a(\Lambda;T=0) + \theta(T - T_f)\left[1 + \{a(\Lambda;T=0) - 1\} \times \left(1 - \frac{T^2 - T_f^2}{T_c^2 - T_f^2}\right)\right], \quad (3.5)$$

where θ is the step function. Although the matching scale Λ can also depend on temperature in hot matter, we assume that it does not have any temperature dependence in the present analysis. Since the Wilsonian matching conditions [see Eqs. (3.1) and (3.2) together with Eq. (2.18)] do not provide a substantial temperature dependence on the ratio $F_\pi(\Lambda;T)/\Lambda$ as well as the parameter $z_3(\Lambda;T)$, we assume that the bare z_3 and bare F_π do not have any T dependences:

$$z_3(\Lambda;T) = z_3(\Lambda;0), \qquad F_\pi(\Lambda;T) = F_\pi(\Lambda;0). \quad (3.6)$$

For making a numerical analysis including hadronic corrections in addition to the intrinsic effects determined above, we take $T_c = 170$ MeV as a typical example and $T_f = 0.7T_c$ as proposed in Refs. [32,33], where the value of T_f is fixed based on the following consideration: The gluon condensate which leads to the trace anomaly in QCD is divided into the soft glue as a mean field and the hard glue as the fluctuation. The soft glue gives spontaneous breaking of scale invariance and the hard glue explicitly breaks it. The anomalous breaking from the quark part is proportional to $m_q\bar{q}q$, with m_q being the current quark mass which indeed vanishes in the classical level if $m_q = 0$. The soft glue melts toward the chiral phase transition point, and eventually the scale invariance is restored at T_c. (Although the scale invariance is still explicitly broken by the hard glue, it has nothing to do with hadron masses.) In Ref. [4] an effective chiral Lagrangian which reproduces the proper scaling behavior even in the level of the EFT was presented and the BR scaling was proposed based on the notion of the melting soft glue. The BR scaling deals with the quantity directly locked to the quark condensate and hence *the scaling masses are achieved exclusively by the intrinsic effect.* According to the lattice calculation [34], the gluon condensate starts to drop around $T = 0.7T_c$ and remains finite at T_c which is about half of that at $T = 0$. The melting soft glue is due to the intrinsic temperature effect which comes in at T_f.

For the bare parameters of the HLS Lagrangian at $T = 0$, we use the ones determined through the Wilsonian matching for $\Lambda_{\rm QCD} = 0.4$ GeV and $\Lambda = 1.1$ GeV ($N_c = 3$ and $N_f = 3$), which well describe [6,24] the experiments at $T = 0$ as briefly shown in Sec. II B. For later convenience, we summarize our input parameters in Table I.

TABLE I. Input parameters in the present analysis. The values listed in the second row are fixed by performing the Wilsonian matching at $T = 0$ with $\langle\bar{q}q\rangle_{1\ \rm GeV} = -(0.25)^3\ \rm GeV^3$ and $\langle\frac{\alpha_s}{\pi}G_{\mu\nu}G^{\mu\nu}\rangle = 0.012\ \rm GeV^4$.

f_π (GeV)	m_ρ (GeV)	$\Lambda_{\rm QCD}$ (GeV)	Λ (GeV)
0.092 46	0.7758	0.4	1.1
$F_\pi(\Lambda)$ (GeV)	$a(\Lambda)$	$g(\Lambda)$	$z_3(\Lambda) \times 10^3$
0.149	1.31	3.63	−2.55
m_π (GeV)	T_c (GeV)	T_f	...
0.139 57	0.17	$0.7T_c$	...

Note that the intrinsic effects also generate the Lorentz noninvariance for the bare parameters and thus the on-shell parameters, which were neglected here since such effects are much suppressed by the matching scale [28]. We show the temperature dependences of the bare parameters g and a in Fig. 3.

Next we incorporate quantum corrections into the parameters following the RGEs at one loop [24]:

$$\mu\frac{dF_\pi{}^2}{d\mu} = \frac{N_f}{2(4\pi)^2}[3a^2g^2F_\pi^2 + 2(2-a)\mu^2],$$
$$\mu\frac{da}{d\mu} = -\frac{N_f}{2(4\pi)^2}(a-1)\left[3a(a+1)g^2 - (3a-1)\frac{\mu^2}{F_\pi^2}\right],$$
$$\mu\frac{dg^2}{d\mu} = -\frac{N_f}{2(4\pi)^2}\frac{87-a^2}{6}g^4,$$
$$\mu\frac{dz_3}{d\mu} = \frac{N_f}{(4\pi)^2}\frac{1+2a-a^2}{12}. \quad (3.7)$$

These parameters are evolved starting from the matching scale toward their on shell and the parameters at the physical scale are obtained. In the following we put a bar over the parameters of the Lagrangian to clarify that the barred quantities include the intrinsic effects and are renormalized at the mass shell of relevant particles: e.g.,

$$\bar{g} = g(\mu = m_\rho;T), \qquad \bar{a} = a(\mu = m_\rho;T),$$
$$\bar{z}_3 = z_3(\mu = m_\rho;T), \qquad \bar{F}_\pi = F_\pi(\mu = 0;T), \quad (3.8)$$
$$\bar{F}_\sigma = \sqrt{\bar{a}}F_\pi(\mu = m_\rho;T), \qquad \bar{M}_\rho = \bar{g}\bar{F}_\sigma.$$

Physical quantities are obtained by including the hadronic corrections generated through thermal loop diagrams at one loop. The hadronic correction to the vector meson mass is given by [7,19][3]

[3]In the following analysis, we include the hadronic thermal corrections only for the leading order parameters, F_π, F_σ, and g. For the calculation of the form factor $\mathcal{F}$, $z_2 - z_1$ is irrelevant. Although $g_\rho(s)$ includes z_3, by which a 30% deviation of experiments from the KSRF I relation can be explained in the vacuum [6,24], we will neglect the hadronic correction to it.

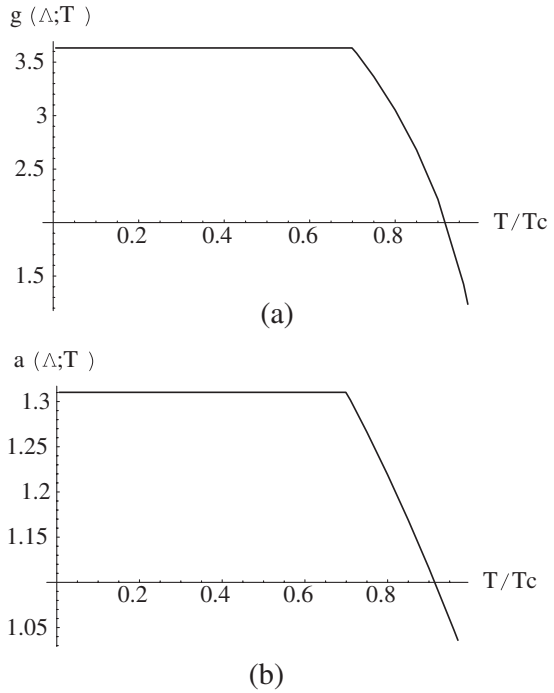

FIG. 3. Temperature dependences of (a) the bare gauge coupling constant g and (b) the bare parameter a.

$$m_\rho^2(T) = \bar{M}_\rho^2 + N_f \bar{g}^2 \Big[-\frac{\bar{a}^2}{12} G_2(\bar{M}_\rho; T) + \frac{5}{4} J_1^2(\bar{M}_\rho; T) + \frac{33}{16} \bar{M}_\rho^2 F_3^2(\bar{M}_\rho; \bar{M}_\rho; T) \Big], \tag{3.9}$$

where the functions J, G, and F are listed in Appendix A, and m_ρ is defined at the rest frame of the ρ meson, $p_\mu = (m_\rho, \vec{0})$.[4]

Differently from a vacuum, the Lorentz invariance is not manifest anymore due to the heat bath. The in-medium pion decay constants, and the temporal and spatial components $f_\pi^{t,s}$ are defined by [35]

$$\langle 0|J_5^0|\pi(p)\rangle = i f_\pi^t p^0, \qquad \langle 0|J_5^i|\pi(p)\rangle = i f_\pi^s p^i, \tag{3.10}$$

where J_5^μ denotes the axial-vector current. The order parameter of the chiral symmetry is defined as the pole residue of the axial-vector current correlator following Ref. [36], which provides $f_\pi^t f_\pi^s$ [27]. On the other hand, the f_π^t is the wave function renormalization constant of the π field [27,37]. The hadronic corrections to two pion-decay constants are [7,19]

$$(f_\pi^t(T))^2 = \bar{F}_\pi^2 - N_f \Big[I_2(T) - \frac{\bar{a}}{\bar{M}_\rho^2} (I_4(T) - J_1^4(\bar{M}_\rho; T)) \Big],$$
$$f_\pi^t(T) f_\pi^s(T) = \bar{F}_\pi^2 - N_f \Big[I_2(T) + a \Big\{ \frac{1}{3\bar{M}_\rho^2} (I_4(T) - J_1^4(\bar{M}_\rho; T)) - J_1^2(\bar{M}_\rho; T) \Big\} \Big], \tag{3.11}$$

where the functions I and J are listed in Appendix A and the soft pion limit for $f_\pi^{t,s}$ was taken.

In general, there are two decay constants for σ (longitudinal ρ). However, they become identical to each other when the bare Lagrangian has the Lorentz invariance:

$$f_\sigma(T)^2 = (f_\sigma^t(T))^2 = f_\sigma^t(T) f_\sigma^s(T) = \bar{F}_\sigma^2 - \frac{N_f}{4} [\bar{a}^2 I_2(T) - J_1^2(\bar{M}_\rho; T) + 2J_{-1}^0(\bar{M}_\rho; T)]. \tag{3.12}$$

As we show in Appendix B [see Eq. (B8)], the momentum-dependent ρ-γ mixing strength is given by

$$g_\rho(s; T) = \bar{g} [f_\sigma^2(T) - s \bar{z}_3], \tag{3.13}$$

where $f_\sigma^2(T)$ includes both intrinsic and hadronic temperature effects as in Eq. (3.12), while $\bar{g}$ and $\bar{z}_3$ include only the intrinsic one.

We show the temperature dependences of the ρ meson mass, $m_\rho(T)$, and the ρ-γ mixing strength at ρ on shell, $g_\rho(s = m_\rho; T)$, in Fig. 4. In this figure the dashed lines show the temperature dependences of the physical quantities when only the hadronic corrections are included, i.e., the parameters of the HLS Lagrangian are assumed to have no temperature dependence. The solid lines show the full temperature dependences by including the intrinsic temperature effects into the bare parameters as given in Eqs. (3.5) and (3.6). Figure 4(a) shows that the vector meson mass including only the hadronic correction changes little with temperature and the hadronic correction gives a positive contribution to m_ρ, $\delta^{(\mathrm{had})} \simeq 5$ MeV. In the temperature region above the flash temperature, $T/T_c > T_f/T_c = 0.7$, the ρ mass with the intrinsic effect rapidly drops corresponding to the rapid decreasing of the gauge coupling as shown in Fig. 3. In Fig. 4(b) we can see that the hadronic effect gives a negative correction to the ρ-γ mixing strength at ρ on shell. This is dominated by the decreasing of f_σ: In the low-temperature region, Eq. (3.12) is approximated as

$$(f_\sigma^t(T))^2 = f_\sigma^t(T) f_\sigma^s(T) \simeq \bar{F}_\sigma^2 - \frac{N_f}{48} \bar{a}^2 T^2, \tag{3.14}$$

for $T \ll m_\rho$. Above the flash temperature, the intrinsic effect causes the rapid drop of the gauge coupling g, which further decreases the g_ρ toward zero.

As we show in the next section and in Appendix B, the $\rho\pi\pi$ and the $\gamma\pi\pi$ couplings appearing in the imaginary

[4]In medium, the full vector meson propagator consists of the longitudinal and tranverse parts, D_L and D_T. The vector meson masses defined as the pole positions of D_L and D_T are identical at the rest frame.

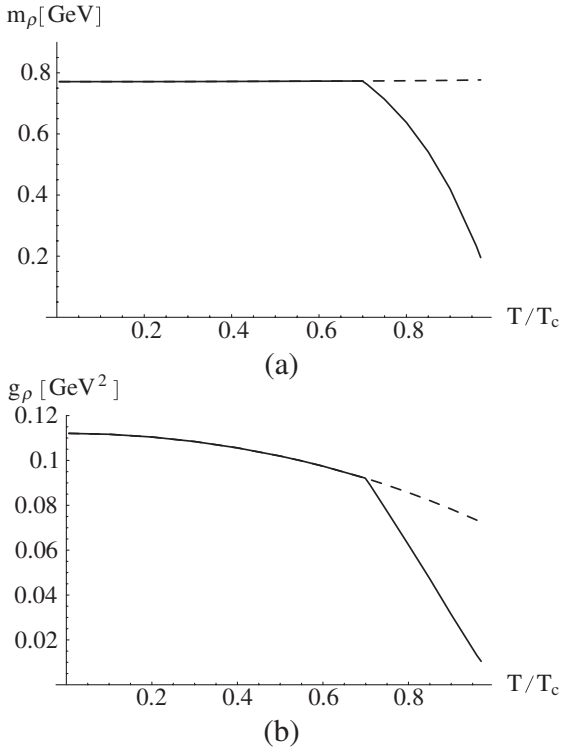

FIG. 4. Temperature dependences of (a) the vector meson mass m_ρ and (b) the ρ-γ mixing strength g_ρ. The solid curves denote the full (both intrinsic and hadronic) temperature dependences. The dashed curves include only the hadronic temperature effects.

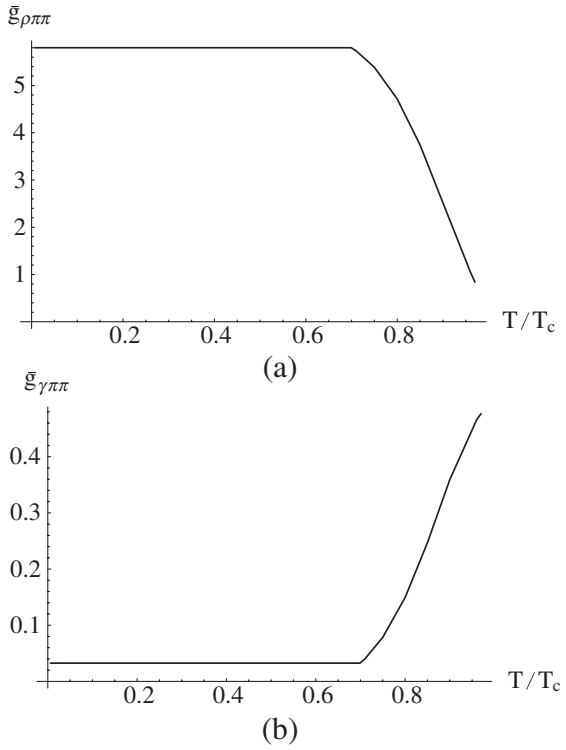

FIG. 5. Temperature dependences of (a) the parametric $\rho\pi\pi$ coupling $\bar{g}_{\rho\pi\pi}$ and (b) the parametric direct-$\gamma\pi\pi$ coupling $\bar{g}_{\gamma\pi\pi}$. The lines denote the temperature dependences including only the intrinsic effects.

part of the photon self-energy do not have the hadronic temperature corrections in the present one-loop calculation. So we need the parametric $\rho\pi\pi$ coupling and the parametric direct-$\gamma\pi\pi$ coupling. By extending the form given in Eqs. (2.12) and (2.13), they are given by

$$\bar{g}_{\rho\pi\pi}(T) = \bar{g}\frac{\bar{a}(0)}{2}, \tag{3.15}$$

$$\bar{g}_{\gamma\pi\pi}(T) = 1 - \frac{\bar{a}(0)}{2}, \tag{3.16}$$

where $\bar{a}(0)$ is defined as [19]

$$\bar{a}(0) = \frac{\bar{F}_\sigma^2}{\bar{F}_\pi^2} = \frac{F_\sigma^2(\mu = m_\rho; T)}{F_\pi^2(\mu = 0; T)}. \tag{3.17}$$

Here we should note that the barred quantities include only the intrinsic effects. In Fig. 5, we show the temperature dependences of $\bar{g}_{\rho\pi\pi}(T)$ and $\bar{g}_{\gamma\pi\pi}(T)$. In Fig. 5(a) the rapid decrease of the parametric $\rho\pi\pi$ coupling $\bar{g}_{\rho\pi\pi}$ occurs above the flash temperature because of the drop of the gauge coupling g caused by the intrinsic effect. Figure 5(b) shows the temperature dependence of the parametric direct-$\gamma\pi\pi$ coupling $\bar{g}_{\gamma\pi\pi}$. In the temperature region below the flash temperature, $\bar{g}_{\gamma\pi\pi}$ is almost zero realizing the VD. Above the flash temperature, the parameter $\bar{a}(0)$ starts to decrease from 2 to 1 due to the intrinsic effect as given in Eq. (3.5). This causes an increase of $\bar{g}_{\gamma\pi\pi}$ toward $1/2$, which implies the strong violation of the VD.

IV. FORM FACTOR AND DILEPTON SPECTRA

A lepton pair is emitted from the hot/dense matter through a decaying virtual photon. The differential production rate in the medium for fixed temperature T is expressed in terms of the imaginary part of the photon self-energy $\mathrm{Im}\Pi$ as

$$\frac{dN}{d^4q}(q_0, \vec{q}; T) = \frac{\alpha^2}{\pi^3 M^2}\frac{1}{e^{q_0/T} - 1}\mathrm{Im}\Pi(q_0, \vec{q}; T), \tag{4.1}$$

where $\alpha = e^2/4\pi$ is the electromagnetic coupling constant, M is the invariant mass of the produced dilepton, and $q_\mu = (q_0, \vec{q})$ denotes the momentum of the virtual photon. The three-momentum integrated rate is given by

$$\frac{dN}{ds}(s; T) = \int \frac{d^3\vec{q}}{2q_0}\frac{dN}{d^4q}(q_0, \vec{q}; T), \tag{4.2}$$

with $s = M^2$ and $q_0 = \sqrt{\vec{q}^2 + M^2}$. We will focus on an energy region around the ρ meson mass scale in this analysis. In this energy region it is natural to expect that the photon self-energy is dominated by the two-pion process, and its imaginary part is related to the pion electromagnetic form factor $\mathcal{F}(s; T)$ through

$$\mathrm{Im}\,\Pi(s;T) = \frac{1}{6\pi\sqrt{s}}\left(\frac{s-4m_\pi^2}{4}\right)^{3/2}|\mathcal{F}(s;T)|^2, \qquad (4.3)$$

with the pion mass m_π. By extending Eq. (2.11) into the in-medium expression, the form factor is written as

$$\mathcal{F}(s;T) = \bar{g}_{\gamma\pi\pi}(T) + \frac{g_\rho(s;T)\cdot\bar{g}_{\rho\pi\pi}(T)}{m_\rho^2(T) - s - \theta(s-4m_\pi^2)im_\rho(T)\Gamma_\rho(s;T)}, \qquad (4.4)$$

where we neglected the temperature dependences of the pion mass. The details are given in Appendix B.

Using the in-medium parameters obtained in the previous section, we calculate the thermal width of the ρ meson. We present the temperature dependence of the width in Fig. 6. The dashed line shows the temperature dependence of Γ_ρ when only the hadronic effect is included. Since $\bar{g}_{\rho\pi\pi}$ is independent of T and m_ρ slightly increases with T as shown in Fig. 4(a) (dashed line), Γ_ρ increases with T which implies that the hadronic effect causes the broadening of the ρ width. The solid line in Fig. 6 shows the temperature dependence of Γ_ρ when the intrinsic effect is also included for $T > T_f$. In this case $\bar{g}_{\rho\pi\pi}$ as well as m_ρ decrease with T as $\bar{g}$ in the VM, and the width Γ_ρ decreases as $\Gamma_\rho \sim \bar{g}^3 \to 0$.

Now, let us calculate the pion form factor and the dilepton production rate. Figure 7 shows the electromagnetic form factor $\mathcal{F}$ given in Eq. (4.4) for several temperatures. In Fig. 7(a) $g_\rho(s)$, m_ρ, and Γ_ρ in the form factor include only the hadronic temperature corrections, and $\bar{g}_{\gamma\pi\pi}$ and $\bar{g}_{\rho\pi\pi}$ have no temperature dependence. There is no remarkable shift of the ρ meson mass but the width becomes broader with increasing temperature, which is consistent with the previous study [38]. In Fig. 7(b) the intrinsic temperature effects are also included into all the parameters in the form factor: $g_\rho(s)$, m_ρ, and Γ_ρ include the intrinsic effect in addition to the hadronic one, and

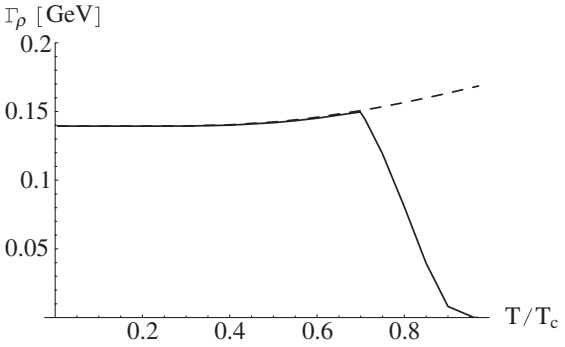

FIG. 6. Decay width of the ρ meson as a function of T/T_c for $\sqrt{s} = m_\rho$. The dashed curve includes only the hadronic temperature effects. The solid curve denotes the full (both intrinsic and hadronic) temperature dependences.

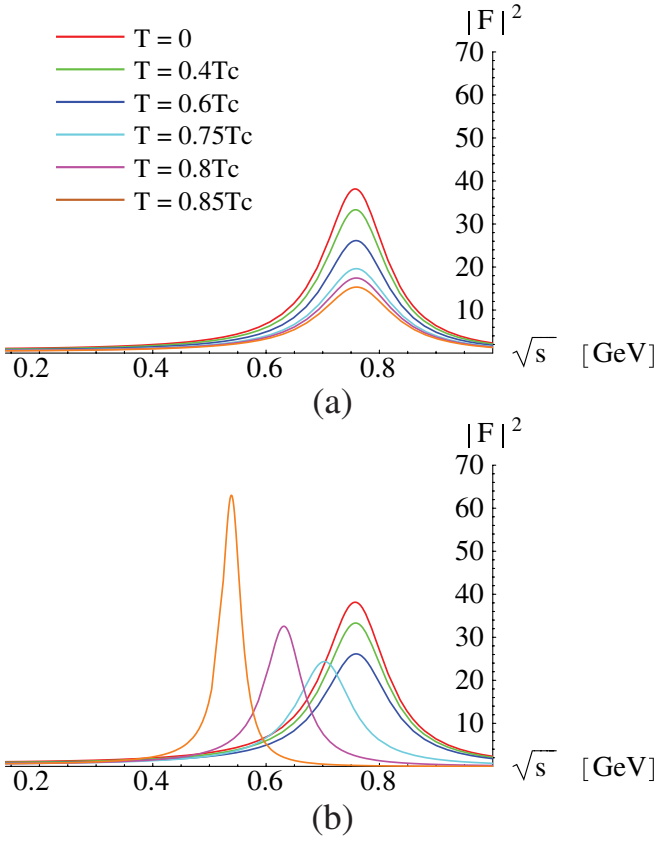

FIG. 7 (color online). Electromagnetic form factor of the pion as a function of the invariant mass $\sqrt{s}$ for several temperatures. The curves in the upper panel (a) include only the hadronic temperature effects and those in the lower panel (b) include both intrinsic and hadronic temperature effects.

$\bar{g}_{\gamma\pi\pi}$ and $\bar{g}_{\rho\pi\pi}$ include the intrinsic one. At the temperature below T_f, the hadronic effect dominates the form factor, so that the curves for $T = 0, 0.4T_c$, and $0.6T_c$ agree with the corresponding ones in Fig. 7(a). At $T = T_f$ the intrinsic effect starts to contribute, and thus in the temperature region above T_f the peak position of the form factor moves as $m_\rho(T) \to 0$ with increasing temperature toward T_c. Associated with this dropping ρ mass, the width becomes narrow, and the value of the form factor at the peak increases as [7]

$$\left|\frac{g_\rho\bar{g}_{\rho\pi\pi}}{m_\rho\Gamma_\rho}\right|^2 \sim \left(\frac{g_\rho}{\bar{g}_{\rho\pi\pi}m_\rho^2}\right)^2 \sim \frac{1}{\bar{g}^2}. \qquad (4.5)$$

As noted in Sec. II C, the VD is controlled by the parameter a in the HLS theory. The VM leads to the strong violation of the VD (indicated by "$\not{\mathrm{VD}}$") near the chiral symmetry restoration point, which can be traced through the Wilsonian matching and the RG evolutions. Thus the direct photon-π-π coupling, $g_{\gamma\pi\pi}$, yields nonvanishing contribution to the form factor together with the ρ meson exchange. When the VD is assumed to be valid even in hot matter, i.e., $g_{\gamma\pi\pi} = 0$, one obtains the following constraint

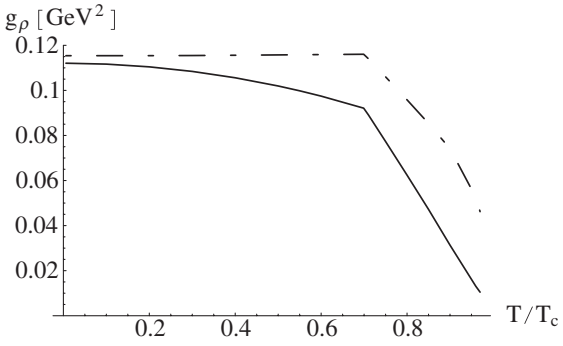

FIG. 8. Temperature dependence of the ρ-γ mixing strength g_ρ for $\sqrt{s} = m_\rho$. The dash-dotted curve corresponds to the case with the VD assumption. The solid curve includes the effect of the VD violation due to the VM.

on g_ρ by imposing the normalization of the electromagnetic charge at $s = 0$:

$$g_\rho^{(\mathrm{VD})}(s;T) = \frac{m_\rho^2(T)}{\bar{g}_{\rho\pi\pi}(T)} - s\bar{g}(T)\bar{z}_3(T). \tag{4.6}$$

Figure 8 shows the temperature dependence of the ρ-γ mixing strength g_ρ at ρ on shell with VD (dash-dotted line) and $\not{\mathrm{VD}}$ (solid line). In the low-temperature region, $T < T_f$, the hadronic corrections to m_ρ and $\bar{g}_{\rho\pi\pi}$ are small, so that the ρ-γ mixing strength with VD, $g_\rho^{(\mathrm{VD})}$, is almost stable against the temperature (see the dash-dotted line), while g_ρ with $\not{\mathrm{VD}}$ gets a non-negligible hadronic correction in the HLS, which causes a decreasing against the temperature (see the solid line). Near the critical temperature, $T > T_f$, on the other hand, both m_ρ and $\bar{g}_{\rho\pi\pi}$ drop due to the VM and the above ratio also decreases since $m_\rho^2/\bar{g}_{\rho\pi\pi} \propto \bar{g}$. However, compared to the g_ρ with $\not{\mathrm{VD}}$, the decreasing of $g_\rho^{(\mathrm{VD})}$ (dash-dotted line) is much more gentle. This affects the pion form factor which exhibits a strong suppression provided by decreasing g_ρ in the VM.

Figure 9 shows the form factor and the dilepton production rate integrated over three-momentum, in which the results with VD and $\not{\mathrm{VD}}$ were compared. The figure shows a clear difference between the curves with VD and $\not{\mathrm{VD}}$. In the low-temperature region, $T \ll T_f$, the hadronic effects are dominant compared with the intrinsic ones, so both curves almost coincide. A difference between them starts to appear around $T = T_f$ and increases with temperature. It can be easily seen that the $\not{\mathrm{VD}}$ gives a reduction compared to the case keeping the VD. The features of the form factor as well as the dilepton production rate coming from two-pion annihilation shown in Figs. 9(a)–9(e) are summarized below for each temperature:

(a) and (b) (below T_f).—The form factor, which has a peak at the ρ meson mass $\sqrt{s} \sim 770$ MeV, is slightly suppressed with increasing temperature. The extent of the suppression in the case with $\not{\mathrm{VD}}$ is greater than that with VD. This is due to the decreasing of the ρ-γ mixing strength g_ρ at finite temperature (see Fig. 8). At $T < T_f$, g_ρ mainly decreases by hadronic corrections. In the case with VD, however, $g_\rho^{(\mathrm{VD})}$ is almost constant. The dilepton rate (a) has two peaks, one is at the ρ meson mass and the other is lying around the low-mass region. The later peak comes from the Boltzman factor of Eq. (4.1). For a rather low temperature the production rate is much enhanced compared with the ρ meson peak since the yield in the higher mass region is suppressed by the statistical factor. With increasing temperature those peaks of the production rate (b) are enhanced and the peak at $\sqrt{s} \sim m_\rho$ clearly appears. In association with decreasing g_ρ, one sees a reduction of the dilepton rate with $\not{\mathrm{VD}}$.

(c), (d), and (e) (above T_f).—Since the intrinsic temperature effects are turned on, a shift of the ρ meson mass to the lower mass region can be seen. Figure 8 shows that g_ρ is further reduced by the intrinsic effects and decreases much more rapidly than $g_\rho^{(\mathrm{VD})}$. Thus the form factor, which becomes narrower with increasing temperature due to the dropping m_ρ, exhibits an obvious discrepancy between the cases with VD and $\not{\mathrm{VD}}$. The production rate based on the VM (i.e., the case with $\not{\mathrm{VD}}$) is suppressed compared to that with the VD. We observe that the suppression is more transparent for larger temperatures: The suppression factor is $\sim$1.8 in (c), $\sim$2 in (d), and $\sim$3.3 in (e).

As one can see in (c), the peak value of the rate predicted by the VM in the temperature region slightly above the flash temperature is even smaller than the one obtained by the vacuum parameters, and the shapes of them are quite similar to each other. This indicates that it might be difficult to measure the signal of the dropping ρ experimentally, if this temperature region is dominant in the evolution of the fireball. In the case shown in (d), on the other hand, the rate by VM is enhanced by a factor of about 2 compared with the one by the vacuum ρ. The enhancement becomes prominent near the critical temperature as seen in (e). These imply that we may have a chance to discriminate the dropping ρ from the vacuum ρ.

V. SUMMARY AND DISCUSSIONS

We studied the pion electromagnetic form factor and the thermal dilepton production rate from the two-pion annihilation within the HLS theory as an effective field theory of low-energy QCD. In the HLS theory the chiral symmetry is restored as the VM in which the massless ρ meson joins the same chiral multiplet as pions. In order to determine the temperature dependences of the parameters of the HLS Lagrangian, the Wilsonian matching to the operator product expansion at finite temperature was made by applying the matching scheme developed in the vacuum [6,24] and at the critical temperature [7,19,27,28].

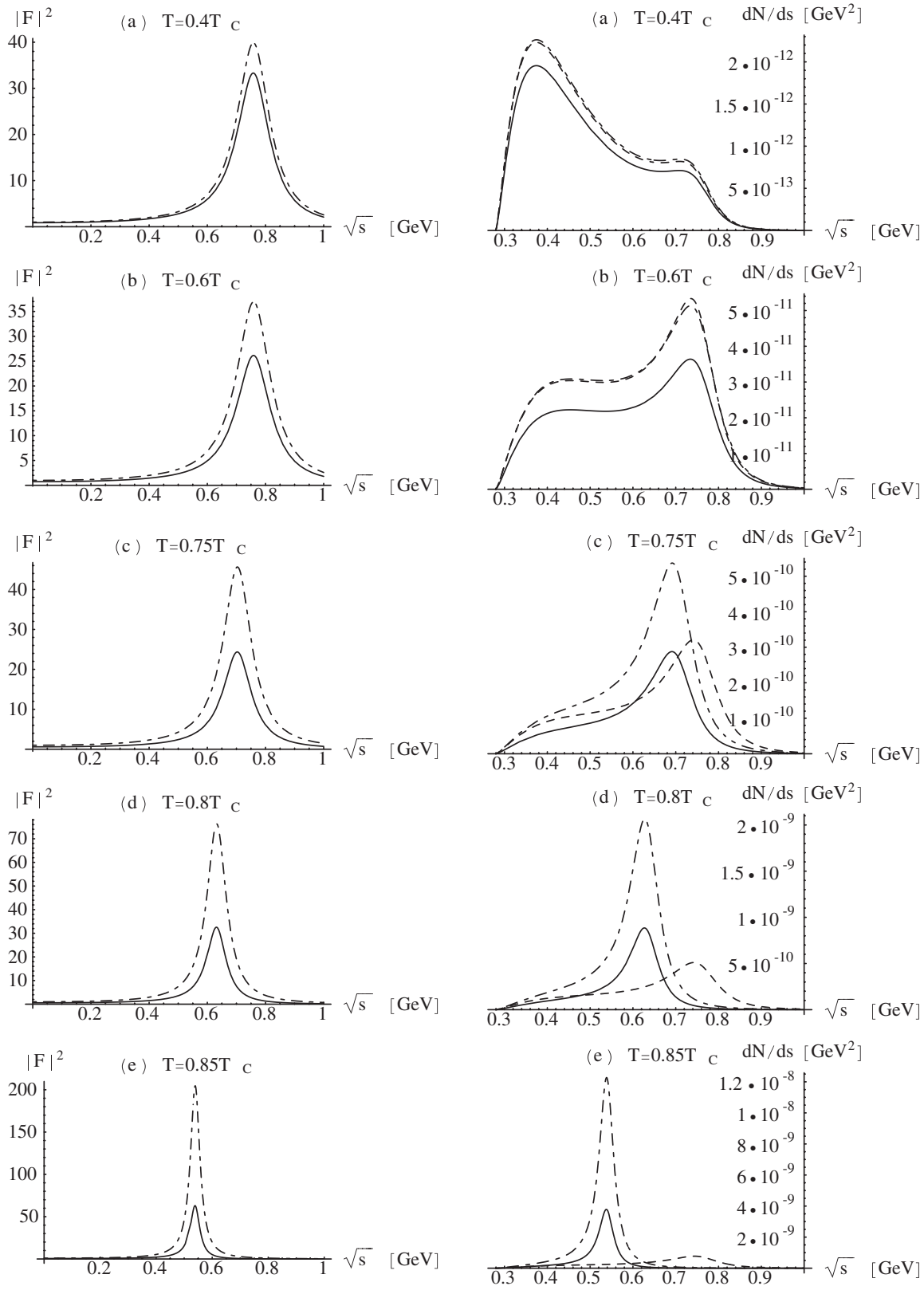

FIG. 9. Electromagnetic form factor of the pion (left) and dilepton production rate (right) as a function of the invariant mass $\sqrt{s}$ for various temperatures. The solid lines include the effects of the violation of the VD. The dash-dotted lines correspond to the analysis assuming the VD. In the dashed lines in the right-hand figures, the parameters at zero temperature were used.

In the Wilsonian matching to define a bare theory in a hot environment, the bare parameters are dependent on temperature, which are referred to as the intrinsic temperature effects. At low temperatures the chiral properties of in-medium hadrons are dominated by ordinary hadronic loop corrections. The dropping ρ is realized in the HLS framework due to the intrinsic effects and thus they play crucial roles especially near the chiral phase transition. In order to see an influence of the intrinsic temperature effects, we presented the form factor including full temperature effects, i.e., the intrinsic and hadronic effects, and compared it with that including only hadronic corrections. The ρ meson mass m_ρ is almost stable against the hadronic corrections and one does not obtain the dropping m_ρ. Accordingly, the peak of the form factor including only the hadronic effects is located at around $\sqrt{s} \sim m_\rho \sim$ 770 MeV even at finite temperature. The form factor is reduced with increasing temperature and, correspondingly, becomes broader. On the other hand, the Wilsonian matching procedure certainly involves the intrinsic temperature effects in the analysis and provides the dropping m_ρ as the VM. The form factor *above the flash temperature* T_f thus starts to present a shift of m_ρ to the lower invariant mass region. Associated with the dropping ρ, the form factor becomes sharp.

One of the significant predictions of the VM is a strong violation of the VD of the pion form factor. The VM predicts that the VD is violated near the transition temperature T_c in which the direct photon-π-π does contribute to the form factor in addition to the ρ meson mediation. It crucially affects the analysis of dilepton yields. We presented the form factor and the dilepton production rate with and without the VD assumption together with the dropping ρ. For $T \ll T_f$ the result shows only a small difference between those two cases since the VD is still well satisfied at low temperatures. A clear difference can be seen for $T > T_f$ where the intrinsic temperature effects contribute to the physical quantities. The form factor and consequently the dilepton production rate, taking account of the violated VD, are reduced and exhibit an obvious difference near T_c compared to those with the VD. Such behaviors can be understood from the in-medium ρ-γ mixing strength g_ρ. At $T \ll T_f$, g_ρ mainly decreases due to the hadronic corrections and does not show a big difference. With increasing temperature but still below T_f, g_ρ shows a discrepancy between the cases with/without the VD, which is roughly 17% around $T = 0.6T_c$. The intrinsic temperature effect comes in at T_f and provides a more rapid decreasing of g_ρ than $g_\rho^{(\mathrm{VD})}$. This variation reaches about 40% at $T = 0.85T_c$ and eventually causes a precise difference of the production rate by a factor $\sim$3.3.

Several comments are in order. The HLS Lagrangian has only pions and vector mesons as physical degrees of freedom, and a time evolution was not considered in this work. Thus it is not possible to make a direct comparison of our results with experimental data. However, a *naive* dropping m_ρ formula, i.e., $T_f = 0$, as well as VD in hot/dense matter are sometimes used for theoretical implications of the data. As we have shown in this paper, the intrinsic temperature effects together with the violation of the VD give a clear difference from the results without including those effects. It may then be expected that a field theoretical analysis of the dropping ρ as presented in this work and a reliable comparison with dilepton measurements will provide evidence for the in-medium hadronic properties associated with the chiral symmetry restoration, if complicated hadronization processes do not wash out those changes.

Our analysis can be applied to a study at finite density. In particular, to study dilepton production rates under the conditions for CERN SPS and future GSI/FAIR should be addressed as an important issue. In such a dense environment, the particle-hole configurations with the same quantum numbers of pions and ρ mesons are crucial [39]. The violation of the VD has also been presented at finite density in the HLS theory [8]. Therefore the dilepton rate as well as the form factor will be much affected by the intrinsic density effects and be reduced above the "flash density."

Recently the chiral perturbation theory including vector and axial-vector mesons as well as pions has been constructed [40,41] based on the generalized HLS [10,42,43]. In this theory the dropping ρ and A_1 meson masses were formulated and it was shown that the dropping masses are related to the fixed points of the RGEs, which gives a VM-type restoration, and that the VD is strongly violated also in this case. Inclusion of the effect of the A_1 meson as well as the effect of collisional broadening will be done in future work.

ACKNOWLEDGMENTS

We are grateful to Gerry Brown, Bengt Friman, and Mannque Rho for fruitful discussions and comments. We also thank Jochen Wambach for stimulating discussions. The work of C. S. was supported in part by the Virtual Institute of the Helmholtz Association under Grant No. VH-VI-041. The work of M. H. is supported in part by the Daiko Foundation (Grant No. 9099), the 21st Century COE Program of Nagoya University provided by Japan Society for the Promotion of Science (Grant No. 15COEG01), and the JSPS Grant-in-Aid for Scientific Research (c) (2) (Grant No. 16540241).

APPENDIX A: FUNCTIONS

In this appendix, we list the integral forms of the functions which appear in the expressions of the hadronic corrections. The functions $I_n(T)$, $J_m^n(M;T)$, $F_3^n(p_0;M;T)$, and $G_n(p_0;T)$ (n, m: integers) are given by

$$
\begin{aligned}
I_n(T) &= \int \frac{d^3k}{(2\pi)^3} \frac{|\vec{k}|^{n-3}}{e^{k/T}-1}, \\
J^n_m(M;T) &= \int \frac{d^3k}{(2\pi)^3} \frac{1}{e^{\omega/T}-1} \frac{|\vec{k}|^{n-2}}{\omega^m}, \\
F^n_3(p_0;M;T) &= \int \frac{d^3k}{(2\pi)^3} \frac{1}{e^{\omega/T}-1} \frac{4|\vec{k}|^{n-2}}{\omega(4\omega^2-p_0^2)}, \\
G_n(p_0;T) &= \int \frac{d^3k}{(2\pi)^3} \frac{|\vec{k}|^{n-3}}{e^{k/T}-1} \frac{4|\vec{k}|^2}{4|\vec{k}|^2-p_0^2},
\end{aligned}
\tag{A1}
$$

where we define

$$
\omega = \sqrt{k^2+M^2}. \tag{A2}
$$

APPENDIX B: IMAGINARY PART OF THE PHOTON SELF-ENERGY

In this appendix, we show the imaginary part of the photon self-energy obtained in the HLS. The photon self-energy used in Sec. IV is related to the vector current correlator in the HLS as

$$
\mathrm{Im}\,\Pi(s) = s\,\mathrm{Im}G_V(s). \tag{B1}
$$

Let $\Pi_V^{\mu\nu}$, $\Pi_{V\parallel}^{\mu\nu}$, and $\Pi_{\parallel}^{\mu\nu}$ denote the V-V, V-$\mathcal{V}$, and $\mathcal{V}$-$\mathcal{V}$ two-point functions, respectively. These two-point functions are decomposed as [6,20]

$$
\Pi^{\mu\nu}(q) = g^{\mu\nu}\Pi^S(q^2) + (g^{\mu\nu}q^2 - q^\mu q^\nu)\Pi^{LT}(q^2). \tag{B2}
$$

By using the two-point functions, the vector current correlator $G_V(s)$ is expressed as [6,20]

$$
G_V = \frac{\Pi_V^S(-\Pi_V^{LT} - 2\Pi_{V\parallel}^{LT})}{\Pi_V^S + s\Pi_V^{LT}} - \Pi_{\parallel}^{LT}. \tag{B3}
$$

By noting that Π_V^S does not have an imaginary part for $s < 4m_\rho^2$ at one loop, the imaginary part of the current correlator is expressed as

$$
\begin{aligned}
\mathrm{Im}G_V = &-\mathrm{Im}\Pi_V^{LT}\frac{(\Pi_V^S - s\,\mathrm{Re}\Pi_{V\parallel}^{LT})^2}{|\Pi_V^S + s\Pi_V^{LT}|^2} \\
&- \mathrm{Im}\Pi_{V\parallel}^{LT}\left[\frac{\Pi_V^S - s\,\mathrm{Re}\Pi_{V\parallel}^{LT}}{\Pi_V^S + s\Pi_V^{LT}} + \frac{\Pi_V^S - s\,\mathrm{Re}\Pi_{V\parallel}^{LT}}{(\Pi_V^S + s\Pi_V^{LT})^*}\right] \\
&- \mathrm{Im}\Pi_{\parallel}^{LT},
\end{aligned}
\tag{B4}
$$

up to higher order terms such as $(\mathrm{Re}\Pi_{V\parallel}^{LT})^2$ and $(\mathrm{Re}\Pi_{V\parallel}^{LT}) \times (\mathrm{Im}\Pi_{V\parallel}^{LT})$.

Using the formulas shown in Refs. [6,20], we obtain

$$
\begin{aligned}
\mathrm{Im}\,\Pi_V^{LT}(s) &= -\frac{1}{48\pi}\left(\frac{s-4m_\pi^2}{s}\right)^{3/2}\left(\frac{\bar{g}_{\rho\pi\pi}}{\bar{g}}\right)^2, \\
\mathrm{Im}\Pi_{V\parallel}^{LT}(s) &= -\frac{1}{48\pi}\left(\frac{s-4m_\pi^2}{s}\right)^{3/2}\bar{g}_{\gamma\pi\pi}\frac{\bar{g}_{\rho\pi\pi}}{\bar{g}}, \\
\mathrm{Im}\Pi_{\parallel}^{LT}(s) &= -\frac{1}{48\pi}\left(\frac{s-4m_\pi^2}{s}\right)^{3/2}(\bar{g}_{\gamma\pi\pi})^2.
\end{aligned}
\tag{B5}
$$

Here $\bar{g}_{\rho\pi\pi}$ and $\bar{g}_{\gamma\pi\pi}$ are expressed by the parameters of the Lagrangian as in Eqs. (2.12) and (2.13). We put a bar over the parameters to clarify that the barred quantities do not include the hadronic temperature corrections and include only the intrinsic effects, when they are considered in hot matter. We define the ρ propagator $D_\rho(s)$ and the momentum-dependent ρ-γ mixing strength $g_\rho(s)$ as

$$
\begin{aligned}
D_\rho(s) &\equiv \frac{1}{\bar{g}^2(\Pi_V^S(s) + s\Pi_V^{LT}(s))}, \\
g_\rho(s) &\equiv \bar{g}(\Pi_V^S(s) - s\,\mathrm{Re}\Pi_{V\parallel}^{LT}(s)).
\end{aligned}
\tag{B6}
$$

In the present analysis, we consider the energy region around the ρ meson mass, $s \sim m_\rho^2$. Then we use the following approximate form for the ρ propagator:

$$
D_\rho(s) \simeq \frac{1}{m_\rho^2 - s - \theta(s-4m_\pi^2)im_\rho\Gamma_\rho}, \tag{B7}
$$

where both m_ρ and Γ_ρ include the hadronic temperature effects in addition to intrinsic ones. We should note that there is not substantial momentum dependence in $\Pi_V^S(s)$ for $s < 4m_\rho^2$, since the pion loop does not contribute to $\Pi_V^S(s)$ except for the tadpole diagram. Then, in the ρ-γ mixing strength $g_\rho(s)$, we take $\Pi_V(s) \to \Pi_V(s=0) = f_\sigma^2$. Furthermore, we neglect the momentum dependence of $\mathrm{Re}\Pi_{V\parallel}^{LT}(s)$ for consistency with the approximation adopted in Eq. (B7). This implies

$$
g_\rho(s) \simeq \bar{g}(f_\sigma^2 - s\bar{z}_3), \tag{B8}
$$

where $\bar{z}_3$ includes the intrinsic temperature effect.

By using the above quantities, the imaginary part of the current correlator $\mathrm{Im}G_V$ in Eq. (B4) is expressed as

$$
\begin{aligned}
\mathrm{Im}G_V(s) = &\frac{1}{48\pi}\left(\frac{s-4m_\pi^2}{s}\right)^{3/2} \\
&\times |\bar{g}_{\gamma\pi\pi} + g_\rho(s)\bar{g}_{\rho\pi\pi}D_\rho(s)|^2,
\end{aligned}
\tag{B9}
$$

which leads to Eq. (4.3).

[1] See, e.g., V. Bernard and U. G. Meissner, Nucl. Phys. **A489**, 647 (1988); T. Hatsuda and T. Kunihiro, Phys. Rep. **247**, 221 (1994); R. D. Pisarski, hep-ph/9503330; F. Wilczek, hep-ph/0003183; G. E. Brown and M. Rho, Phys.

Rep. **363**, 85 (2002).
[2] R. Rapp and J. Wambach, Adv. Nucl. Phys. **25**, 1 (2000).
[3] G. Agakishiev *et al.* (CERES Collaboration), Phys. Rev. Lett. **75**, 1272 (1995).
[4] G. E. Brown and M. Rho, Phys. Rev. Lett. **66**, 2720 (1991).
[5] M. Harada and K. Yamawaki, Phys. Rev. Lett. **86**, 757 (2001).
[6] M. Harada and K. Yamawaki, Phys. Rep. **381**, 1 (2003).
[7] M. Harada and C. Sasaki, Phys. Lett. B **537**, 280 (2002).
[8] M. Harada, Y. Kim, and M. Rho, Phys. Rev. D **66**, 016003 (2002).
[9] M. Bando, T. Kugo, S. Uehara, K. Yamawaki, and T. Yanagida, Phys. Rev. Lett. **54**, 1215 (1985).
[10] M. Bando, T. Kugo, and K. Yamawaki, Phys. Rep. **164**, 217 (1988).
[11] K. Ozawa *et al.* (E325 Collaboration), Phys. Rev. Lett. **86**, 5019 (2001); S. Yokkaichi, in Proceedings of the International Workshop on Chiral Restoration in Nuclear Medium, RIKEN, Japan, 2005 (http://chiral05.riken.jp/); M. Naruki *et al.*, Phys. Rev. Lett. **96**, 092301 (2006).
[12] D. Trnka *et al.* (CBELSA/TAPS Collaboration), Phys. Rev. Lett. **94**, 192303 (2005).
[13] E. V. Shuryak and G. E. Brown, Nucl. Phys. **A717**, 322 (2003).
[14] S. Damjanovic *et al.* (NA60 Collaboration), J. Phys. G **31**, S903 (2005).
[15] S. Damjanovic *et al.* (NA60 Collaboration), Nucl. Phys. **A774**, 715 (2006).
[16] G. E. Brown and M. Rho, nucl-th/0509001; nucl-th/0509002.
[17] H. van Hees and R. Rapp, hep-ph/0604269.
[18] B. Schenke and C. Greiner, hep-ph/0608032.
[19] M. Harada and C. Sasaki, Nucl. Phys. **A736**, 300 (2004).
[20] C. Sasaki, Doctoral thesis, Nagoya University, hep-ph/0504073.
[21] M. Harada and K. Yamawaki, Phys. Lett. B **297**, 151 (1992).
[22] H. Georgi, Phys. Rev. Lett. **63**, 1917 (1989); Nucl. Phys. **B331**, 311 (1990).
[23] M. Tanabashi, Phys. Lett. B **316**, 534 (1993).
[24] M. Harada and K. Yamawaki, Phys. Rev. D **64**, 014023 (2001).
[25] T. Fujimori, M. Harada, and C. Sasaki (unpublished).
[26] M. A. Shifman, A. I. Vainshtein, and V. I. Zakharov, Nucl. Phys. **B147**, 385 (1979); **B147**, 448 (1979).
[27] M. Harada, Y. Kim, M. Rho, and C. Sasaki, Nucl. Phys. **A727**, 437 (2003).
[28] C. Sasaki, Nucl. Phys. **A739**, 151 (2004); M. Harada, Y. Kim, M. Rho, and C. Sasaki, Nucl. Phys. **A730**, 379 (2004); M. Harada, M. Rho, and C. Sasaki, hep-ph/0506092.
[29] M. Harada, M. Rho, and C. Sasaki, Phys. Rev. D **70**, 074002 (2004).
[30] M. Harada and K. Yamawaki, Phys. Rev. Lett. **87**, 152001 (2001).
[31] J. J. Sakurai, *Currents and Mesons* (University of Chicago Press, Chicago, 1969).
[32] G. E. Brown, C. H. Lee, and M. Rho, Phys. Rev. C **74**, 024906 (2006).
[33] G. E. Brown, C. H. Lee, and M. Rho, Nucl. Phys. **A747**, 530 (2005).
[34] D. E. Miller, hep-ph/0008031.
[35] R. D. Pisarski and M. Tytgat, Phys. Rev. D **54**, R2989 (1996).
[36] A. Bochkarev and J. Kapusta, Phys. Rev. D **54**, 4066 (1996).
[37] U. G. Meissner, J. A. Oller, and A. Wirzba, Ann. Phys. (N.Y.) **297**, 27 (2002).
[38] C. Song and V. Koch, Phys. Rev. C **54**, 3218 (1996).
[39] B. Friman and H. J. Pirner, Nucl. Phys. **A617**, 496 (1997).
[40] M. Harada and C. Sasaki, Phys. Rev. D **73**, 036001 (2006).
[41] Y. Hidaka, O. Morimatsu, and M. Ohtani, Phys. Rev. D **73**, 036004 (2006).
[42] M. Bando, T. Kugo, and K. Yamawaki, Nucl. Phys. **B259**, 493 (1985).
[43] M. Bando, T. Fujiwara, and K. Yamawaki, Prog. Theor. Phys. **79**, 1140 (1988).
[44] L. M. Barkov *et al.*, Nucl. Phys. **B256**, 365 (1985).
[45] R. R. Akhmetshin *et al.* (CMD-2 Collaboration), Phys. Lett. B **578**, 285 (2004).